Research Journal of Applied Sciences 9 (6): 314-319, 2014
ISSN: 1815-932X

Design, Simulation and Characterization of Piezoelectric Stack Actuator MEMS Based Microdroplet Ejector

[1]K. Ganesan and [2]V. Palanisamy
[1]Anna University, Chennai, Tamilnadu, India
[2]Info Institute of Engineering, Coimbatore, Tamilnadu, India

Abstract: In this study, researchers present the design, analysis and fabrication of MEMS based silicon micro-needles for insertion of fluid into the dermis and subcutaneous fat layer of human skin. Microelectromechanical Systems (MEMS) are uncovered to an assortment of liquid environments in applications such as chemical and biological sensors and microfluidic devices. In this study, the design and fabrication of a multi-material high-performance micropump is presented. The fabrication process using MEMS fabrication techniques, comprised of silicon and pyrex micromachining and bonding. Manufacturing steps such as three small bulk cylindrical piezoelectric material elements that are integrated with micro-fabricated Silicon-On-Insulator (SOI) and glass micromachined substrates using eutectic bonding and anodic bonding processes were successfully realized and provide a robust and scalable production technique for the micro pump. Exceptional flow rates of 0.1 mL min^{-1} with 1 W power consumption based on piezoelectric stack actuation achieved by appropriate design optimization. The analysis forecasts that the resultant stresses due to applied meandering and axial loads are in the safe range below the acquiesce strength of the material.

Key words: MEMS, SOI, pyrex micromachining, eutectic bonding, anodic bonding

INTRODUCTION

There are many advantages to miniaturizing systems for chemical and biological analysis (Ashraf *et al*., 2011). Recent interest in this area has led to the creation of several research programs including a Micro Gas Analyzer (Jiang *et al*., 2002). The aim of this project is to develop a new approach for detecting biological and chemical agents. Currently available portable drug delivery micropump (Mousoulis *et al*., 2011) are expensive, slow, bulky and consume significant power. New approaches that have the potential for instantaneous detection in the field that are low cost, portable and consume very little power would be extremely useful. The possible advantages and applications of such a device are numerous: it could be deployed in remote locations in laboratories and industry for chemical and biological agent analysis or as safety leakage detectors and of course in the field in the hand or on the uniform of an inspector or intelligent robot that is able to communicate with a base station. The Micro Gas Analyzer (Wu *et al*., 2008) will consist of several key components that will themselves also be very useful in other areas of research as well as find applications in industry.

This research work will focus on demonstrating that a MEMS Micro Vacuum Pump to meet the specifications can be made these specifications call for the generation of 0.1 mL min^{-1} flow rate with 1 W power consumption based on piezoelectric stack actuation (Percin and Kuri-Yakub, 2002). Typical large-scale instruments operate at rather low pressures ($<\mu N/m^2$) because of the requirement that ions suffer few collisions during mass analysis. One of the first micropumps was developed by Jan Smits in the early 1980s for use in insulin delivery systems (Zordan *et al*., 2010). Since, then micropumps have been developed for medical applications, microelectronic device cooling and chemical and biological analysis among other applications (e.g., space exploration) (Chevalier and Ayela, 2008). The two main types of pumps are:

- Displacement pumps: in which boundaries moving the fluid create pressure differentials
- Dynamic pumps: in which energy is added to the fluid to increase its momentum or its pressure

The typical reciprocating displacement micropump with a pump chamber and diaphragm, an actuator and two passive check valves at the chamber input and output. When the diaphragm is actuated to increase the pump chamber volume fluid (Evans and Gianchandani, 2010) is sucked into the pump and when the diaphragm is actuated to decrease the pump chamber volume fluid is pushed out of the pump. Check valves open and close depending on the pressure differential across them and the direction of fluid flow is shown in the Fig. 1.

Corresponding Author: K. Ganesan, Anna University Chennai, Tamilnadu, India

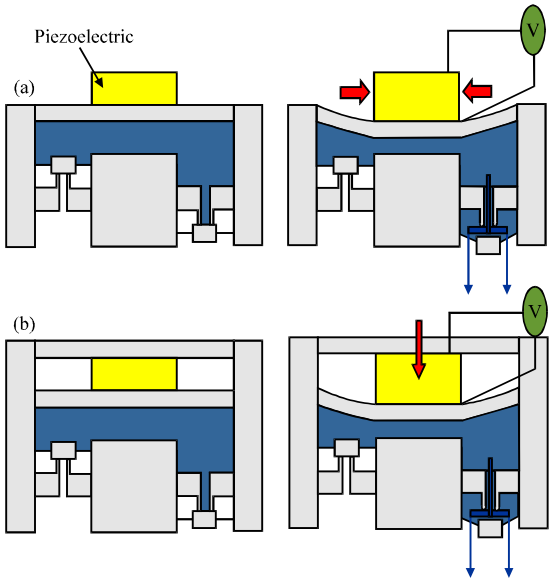

Fig. 1: a) Piezoelectric actuator in the lateral-strain configuration; b) Piezoelectric actuator in the axial strain configuration

MICROPUMP DESIGN

To meet the goals for speed, power and vacuum generation the appropriate choice was to use an active valve reciprocating displacement micropump design (Santra *et al*., 2002). The majority of micro-valves are classified as either active or passive. Passive valves (also called check valves) are not actuated by an external control unit they are opened by pressure differentials and the direction of through-flow and are mostly mechanical flap structures (Jang *et al*., 2007) or flexible diaphragms.

The micropump design consists of 5 layers (i.e., 5 wafers) but layers 1-3 define the ultimate performance since they contain the channels, chambers, pistons and tethers connecting the pistons to the side walls. The aim of this thesis is to focus on the design and fabrication of these layers for testing. Layer 4 contains the piezos (Ashraf *et al*., 2010) to drive the pistons and layer 5 provides structural support (Zhang *et al*., 2002) both of which can be integrated to make the final device once a suitable design for layers 1-3 is found.

There are three main parts to the test setup: the fluidic connections (Kaneda and Fujii, 2010), electronics and circuitry and computer software. Researchers begin by looking at the fluidic connections. The micropump dies to be tested are clamped using optical clamps (Jang *et al*., 2009) onto the testing platform. Each pump die has 5 access ports: one input port, one output port (interchangeable) and three actuation ports (Han *et al*., 2006) for the input/output valves and the pump chamber. O-rings (Wester *et al*., 2009) help seal the pump die ports against the testing platform. The final process flow corresponds to a set of 8 masks and the CAD (Nisar *et al*., 2008) layout shown in Fig. 2.

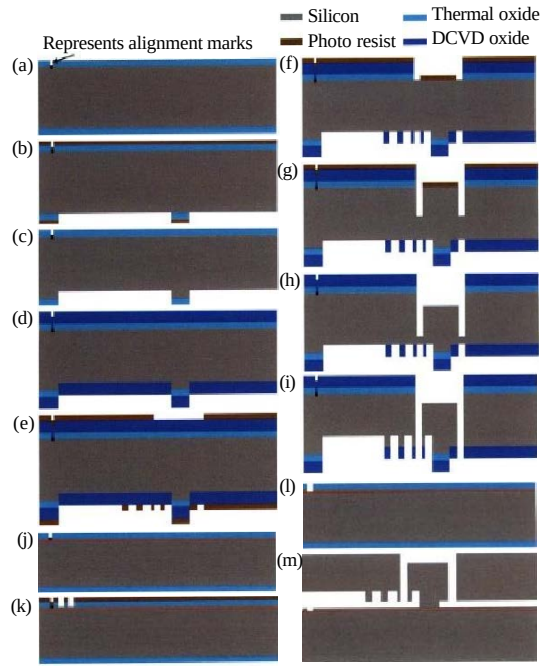

Fig. 2: a-m) Different CAD layout of the micropump layer

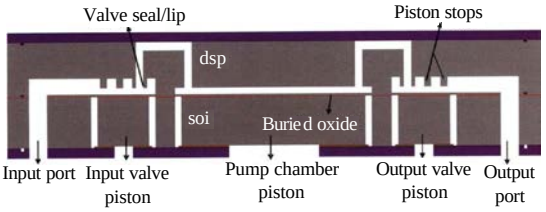

Fig. 3: DSP layer

MEMS micropump layer design

Layer 2-DSP (450 um Si (Fig. 3)):

- Grow thermal oxide (0.3 um)-preferably buy wafers with thermal oxide pre-grown (Loverich *et al*., 2006)
- HMDS wafers, deposit thin resist on both sides, pre-bake, photo M1 (alignment marks) on topside, develop, post-bake
- BOE for 4 min, spin-dry wafers
- Alignment mark etch topside using Almark recipe on STS2 or STS3 for 10 sec
- Strip resist using piranha, spin-dry wafers
- HMDS wafers, deposit thin resist on both sides, pre-bake, photo M1 (alignment marks) on bottomside making sure they line up with topside alignment marks, develop, post-bake

- BOE for 4 min, spin-dry wafers
- Alignment mark etch bottomside using Almark recipe on STS2 or STS3 for 10 sec
- HMDS wafers, deposit thin resist on both sides, pre-bake, photo M3 (6 um chamber etch) on bottomside, develop, postbake
- BOE for 4 min, spin-dry wafers
- Etch pump chamber from bottom using Jbetch in STS3 till 6 um chamber depth is obtained (measure using dektak profilometer) (Sbiaa, 2006), rotate wafers at least 4 times during etch
- Strip resist using piranha, spin-dry wafers
- Deposit 4 um of thick oxide on both sides using ICL DCVD
- HMDS wafers, deposit thick resist on both sides, pre-bake, photo M5 (valve lip and posts) on bottomside, photo M3 (cross channels) on topside, develop, post-bake
- Etch 4.3 um of oxide on both sides using ICL AME5000
- Strip resist using piranha, spin-dry wafers
- HMDS wafers, deposit thick resist on both sides, pre bake, photo M4 (through holes) on topside, develop, post bake
- Etch through holes from the top by (450-30-channel width) microns using recipe MIT69A on STS2, make sure to rotate wafers often for etch uniformity
- Strip resist using piranha, spin-dry wafers
- Ash wafers for 1.5 h
- HMDS wafers, deposit thick resist on bottomside, post-bake
- Etch through holes and channels from the top by the channel width microns making sure to stop short of ~24 um of breaking through the bottomside using recipe MIT69A on STS2, make sure to rotate wafers often for etch uniformity
- Strip resist using piranha, spin-dry wafers
- HMDS wafers, deposit thin resist on topside, post-bake
- Apply blue-tape to topside
- Etch from the bottom by slightly >24 um to create the valve lips, support posts and open up the valve to pump chamber channels. Use recipe MIT69A on STS2, make sure to rotate wafers often for etch uniformity
- Once complete place wafer in acetone till blue-tape comes off
- Strip resist using piranha, spin-dry wafers
- Ash wafers for 1.5 h

Layer 3-SOI (450 um Si) (Fig. 4):

- Grow thermal oxide (0.3 um)-preferably buy wafers with thermal oxide pre-grown

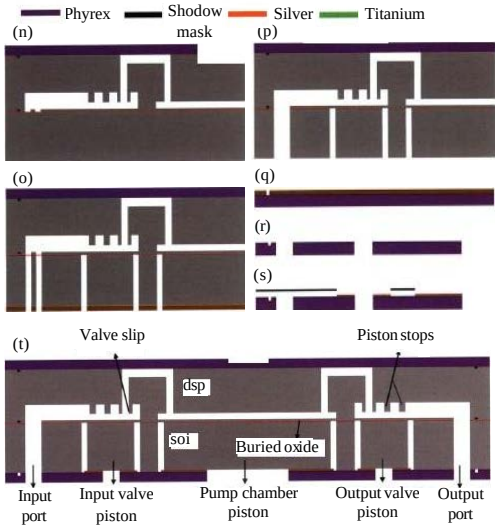

Fig. 4: n-t) Different layout of the micropump SOI layer

- HMDS wafers, deposit thin resist on both sides, pre-bake, photo M1 (alignment marks) on topside, develop, post-bake
- BOE for 4 min, spin-dry wafers
- Alignment mark etch topside using Almark recipe on STS2 or STS3 for 10 sec
- Strip resist using piranha, spin-dry wafers
- HMDS wafers, deposit thin resist on both sides, pre-bake, photo M1 (alignment marks) on bottom side making sure they line up with topside alignment marks, develop, post-bake
- BOE for 4 min, spin-dry wafers
- Alignment mark etch bottom side using A1 mark recipe on STS2 or STS3 for 10 sec
- HMDS wafers, deposit thin resist on both sides, pre-bake, photo M7 (input/output ports) on topside, develop, post bake
- BOE for 4 min, spin-dry wafers
- Etch input/output ports from the top by 10 um until the buried oxide layer is reached using recipe MIT69A in STS2, rotate wafers at least 4 times during etch
- Strip resist using piranha, spin-dry wafers
- Deposit 4 um of thick oxide on the bottom side using ICL DCVD
- HMDS wafers, deposit thick resist on both sides, pre-bake, photo M6 (tethers) on Bottom side, develop, post-bake
- Etch 4.3 um of oxide on bottom side using ICL AME5000
- Strip resist using piranha, spin-dry wafers

- HMDS wafers, deposit thin resist on topside, post-bake
- Apply blue-tape to topside
- Etch tethers from the bottom till the buried oxide is reached and the right tether width/fillet profile is obtained. Use recipe MIT69A on STS2. Make sure to rotate wafers often for etch uniformity. Once any tether is complete paint it with resist by hand and let it dry in air for 3 h before proceeding with etching other tethers-don't use oven
- Once tethers all completed place wafer in acetone till blue-tape comes off
- Strip resist using piranha, spin-dry wafers
- Ash wafers for 1.5 h

Bottom support pyrex layer:

- Get alignment marks, input/output and actuation ports machined by Bullen Ultrasonics (Kan *et al*., 2005) using M8 (pyrex holes)

- Make a shadow mask for the pyrex wafer: HMDS a blank Si wafer, deposit double layer of thick resist on the topside, pre-bake, photo M9 (shadow mask) on topside, develop, post-bake, mount on quartz wafer and etch through the wafer till the shadow mask is complete using recipe Jbetch on STS2 or STS3
- Un amount shadow mask from quartz wafer and clean using piranha then spin-dry wafers (Maillefer *et al*., 2001). Align shadow mask to quartz wafer using bonding aligner and water droplets (to help wafers stick together)
- Deposit 0.02 um of titanium adhesive layer followed by 0.2 um of silver in Ebeam (Selam, 2001)

Bonding and cutting:

- HF strip all oxide from DSP layer 2
- BOE strip all oxide from SOI layer 3 at the same time the buried oxide will also be removed (don't etch more than buried oxide thickness so make sure that all other oxide on the wafer is already thinner before beginning this step). Can't use HF on this layer
- Spin dry clean the pyrex bottom layer
- RCA clean layer 2, 3 and a blank capping Si wafer (no HF)
- Silicon direct bond blank capping wafer to layer 2-3
- Anneal the 3 layer silicon stack for 1 h at 950° Celcius
- Anodically bond stack to pyrex bottom layer
- Die-saw the micropump dies using thickest black blade (use die-saw tape on both sides to prevent water/slurry from entering the devices)

RESULTS AND HYPOTHESIS

This round of fabrication led to a fully functioning set of vacuum micropumps. Using the test setup, researchers performed the main set of tests on these devices:

- Test 1: check for valve and pump chamber leaks by actuating the pistons and measuring any flows at the Input or output ports
- Test 2: check that all pistons can shut down flow by applying an external pressure source at the input and measuring the flow rate at the output as each of the pistons is actuated
- Test 3: measure the flow rate through the device as a function of the pressure differential applied across it
- Test 4: measure the micropump generated flow rate via the 6 stage pumping cycle shown as a function of operating frequency
- Test 5: measure the micropump generated vacuum at a frequency of operation in the micropump's operating range indicated by test 4

PUMP MODELS AND CHARACTERIZATION

To test the pistons, researchers applied a constant pressure source at the input port and measured the output flow rate using a mass flow meter as we attempted to actuate the pistons. Researchers only applied positive pressures to actuate the pistons (no vacuum to pull them down). Ideally for actuation pressures above the input pressure, the pistons should actuate shut and the output flow should drop to.

Air is input at the input port and the output flow rate is measured using a flow sensor. As the three pistons are actuated (indicated by the transparent vertical bars), researchers expect to see a complete cut off any flow (green data for the input piston, red for the chamber piston and blue for the output piston). Note that the input and output pistons do work to some degree but that the pump chamber tether is leaking air is shown in Fig. 5 and 6.

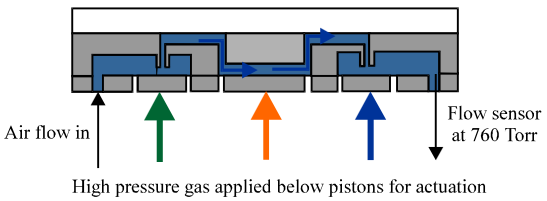

Fig. 5: Layout of the micropump flow model

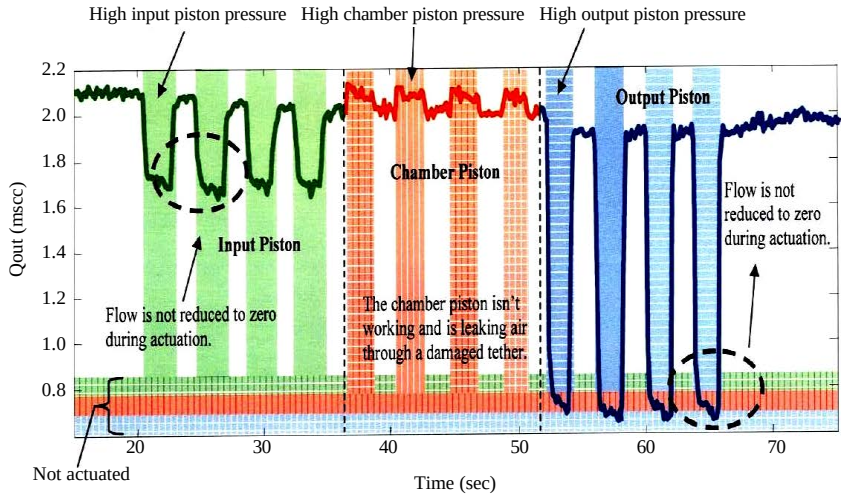

Fig. 6: Simulation results of high pressure flow in the micropump

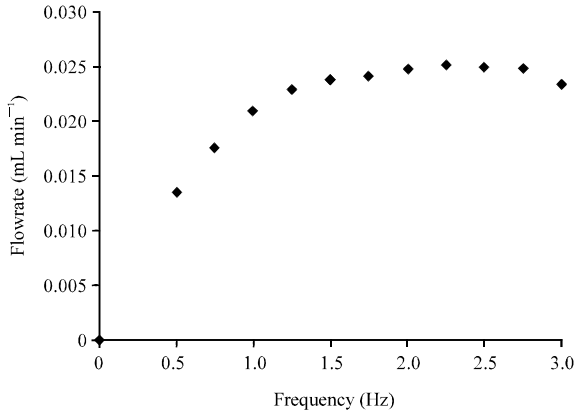

Fig. 7: Simulation results of cumulative flow rate as a function of the frequency

SIMULATION RESULT

The measured flow rate as a function of the operating frequency (6 stage pumping cycle) is plotted in Fig. 7 which gives the exceptional flow rates of 0.25 mL min^{-1} based on piezoelectric stack actuation.

CONCLUSION

This air micropumps is the most effective model. Coventorware Software tool used for the analysis of plate/thin film bending/stress and for fluid flow in MEMS devices. It is a complete pneumatic testing platform and effective testing techniques for the characterization of micropump devices. This experimental data demonstrating how the various design parameters influence pump and valve performance. Finally, an attractive design that would bring us closer to meet the micropump for drug delivery system goals. Valve leakage data for various valve designs was collected and compared with various models. This micro pump capable of generating vacuum below atmosphere and which was demonstrated at different frequency operation. This pump may be designed pneumatically-driven with self contained actuation.

REFERENCES

Ashraf, M.W., S. Tayyaba and N. Afzulpurkar, 2011. Micro Electromechanical Systems (MEMS) based microfluidic devices for biomedical applications. Int. J. Mol. Sci., 12: 3648-3704.

Ashraf, M.W., S. Tayyaba, A. Nisar, N. Afzulpurkar and D.W. Bodhale *et al.*, 2010. Design, fabrication and analysis of silicon hollow microneedles for transdermal drug delivery system for treatment of hemodynamic dysfunctions. Cardiovasc. Eng., 10: 91-108.

Chevalier, J. and F. Ayela, 2008. Microfluidic on chip viscometers. Rev. Scient. Instrum., Vol. 79. 10.1063/1.2940219

Evans, A.T. and Y.B. Gianchandani, 2010. Note: A low leakage liquid seal for micromachined gas valves. Rev. Scient. Instrum., Vol. 81. 10.1063/1.3436642.

Han, A., N.F. de Rooij and U. Staufer, 2006. Design and fabrication of nanofluidic devices by surface micromachining. Nanotechnology, 17: 2498-2503.

Jang, L.S., K. Shu, Y.C. Yu, Y.J. Li and C.H. Chen, 2009. Effect of actuation sequence on flow rates of peristaltic micropumps with PZT actuators. Biomed. Microdevices, 11: 173-181.

Jang, L.S., Y.J. Li, S.J. Lin, Y.C. Hsu, W.S. Yao, M.C. Tsai and C.C. Hou, 2007. A stand-alone peristaltic micropump based on piezoelectric actuation. Biomed. Microdevices, 9: 185-194.

Jiang, L., J. Mikkelsen, J.M. Koo, D. Huber and S. Yao *et al*., 2002. Closed-loop electro osmotic micro channel cooling system for VLSI circuits. Proceedings of the IEEE Transactions on Components and Packaging Technologies, Volume 253, September 2002, Stanford University, USA., pp: 47-55.

Kan, J., M. Xuan, Z. Yang, Y. Wu, B. Wu and G. Cheng, 2005. Analysis and test of piezoelectric micropump for drug delivery. Sheng Wu Yi Xue Gong Cheng Xue Za Zhi, 4: 809-813.

Kaneda, S. and T. Fujii, 2010. Integrated microfluidic systems. Nano/Micro Biotechnol., 119: 179-194.

Loverich, J.J., I. Kanno and H. Kotera, 2006. Concepts for a new class of all-polymer micropumps. Lab Chip, 6: 1147-1154.

Maillefer, D., S. Gamper, B. Frehner, P. Balmer, H. van Lintel and P. Renaud, 2001. A high-performance silicon micropump for disposable drug delivery systems. Proceedings of the 14th IEEE International Conference on Digital Object Identifier, Micro Electro Mechanical Systems, January 21-25, 2001, Interlaken, pp: 413-417.

Mousoulis, C., M. Ochoa, D. Papageorgiou and B. Ziaie, 2011. A skin-contact-actuated micropump for transdermal drug delivery. IEEE Trans. Biomed. Eng., 58: 1492-1498.

Nisar, A., N. Afzulpurkar, A. Tuantranont and B. Mahaisavariya, 2008. Three dimensional transient multifield analysis of a p iezoelectric micropump for drug delivery system for treatment of hemodynamic dysfunctions. Cardiovasc. Eng., 8: 203-218.

Percin, G. and B.T. Khuri-Yakub, 2002. Piezoelectrically actuated flextensional micromachined ultrasound droplet ejectors. Proceedings of the IEEE Transactions on Ultrasonics, Ferroelectrics and Frequency Control, June 2002, Los Altos, CA, pp: 756-766.

Santra, S., P. Holloway and C.D. Batich, 2002. Fabrication and testing of a magnetically actuated micropump. Sensors Actuators B: Chem., 873L: 358-364.

Sbiaa, Z., 2006. MEMS fabricated chip for an implantable drug delivery device. Proceedings of the 28th Annual International Conference of the IEEE Engineering in Medicine and Biology Society, August 30-September 3, 2006, New York, pp: 5621-5624.

Selam, J.L., 2001. External and implantable insulin pumps: Current place in the treatment of diabetes. Exp. Clin. Endocrinol. Diabete, 109: S333-S340.

Wester, B.A., J.D. Ross, S. Rajaraman and M.G. Allen, 2009. Packaging and characterization of mechanically actuated microtweezers for biomedical applications. Proceedings of the Annual International Conference of the IEEE Engineering in Medicine and Biology Society, September 3-6, 2009, Minneapolis, MN., pp: 2744-2747.

Wu, M.H., S.B. Huang, Z. Cui and G.B. Lee, 2008. A high throughput perfusion-based microbioreactor platform integrated with pneumatic micropumps for three-dimensional cell culture. Biomed. Microdevices, 10: 309-319.

Zhang, L., J.M. Koo, L. Jiang, M. Asheghi, K.E. Goodson, J.G. Santiago and T.W. Kenny, 2002. Measurements and modeling of two-phase flow in microchannels with nearly constant heat flux boundary conditions. J. Microelectromech. Syst., 11: 12-19.

Zordan, E., F. Amirouche and Y. Zhou, 2010. Principle design and actuation of a dual chamber electromagnetic micropump with coaxial cantilever valves. Biomed. Microdevices, 12: 55-62.